Biomechanical response of lumbar intervertebral disc in daily sitting postures

Title Page

Biomechanical Response of Lumbar Intervertebral Disc in Daily Sitting Postures: A Poroelastic Finite Element Analysis

Liang-dong Zheng[a,1], Yu-ting Cao [a,1], Yi-ting Yang [a,1], Meng-lei Xu[a], Hui-zi Zeng[a], Shi-jie Zhu[a], Antonio Candito[b], Yuhang Chen[b,*], Rui Zhu[a,*], Li-ming Cheng[a]

[a] *Key Laboratory of Spine and Spinal Cord Injury Repair and Regeneration of Ministry of Education, Tongji Hospital, School of Medicine, Tongji University, Shanghai 200065, China*

[b] *Institute of Mechanical, Process and Energy Engineering, School of Engineering and Physical Sciences, Heriot-Watt University, United Kingdom, EH14 4AS*

[1] *These authors contribute equally to this paper.*

* Corresponding author:

* Dr. Rui Zhu

Key Laboratory of Spine and Spinal Cord Injury Repair and Regeneration（Tongji University）, Ministry of Education

389 Xincun Road

200065 Shanghai

China

E-mail: zhurui08@hotmail.com

* Dr. Yuhang Chen

School of Engineering and Physical Sciences, Heriot-Watt University, United Kingdom, EH14 4AS

E-mail: y.chen@hw.ac.uk

Word Count: 225 (Abstract), 3538 (Main text)

Figures: 5

Tables: 1

Abstract

Background: Prolonged sitting in poor posture has an adverse effect on the lumbar spine. However, the effect of different sedentary behaviors on the intervertebral disc degeneration is less known. This study aims to evaluate the effect of different sitting postures and their durations on the mechanical responses of the disc.

Method: A 3D poroelastic L4–L5 finite element model was established and validated. The parameters of disc height loss, fluid loss in the nucleus pulposus, intradiscal pressure and von-Mises stress in the inter-lamellar matrix were predicted in standing, upright sitting, flexed sitting and extended sitting for duration of 8 hours.

Results: During the sustained loading conditions, the height loss, fluid loss and von-Mises stress gradually increased, but the intradiscal pressure decreased. The varying rates of aforementioned parameters were more significant at the initial loading stage and less so at the end. The predicted values in the flexed sitting posture were significantly greater than other postures. The extended sitting posture caused an obvious von-Mises stress concentration in the posterior region of the inter-lamellar matrix.

Conclusions: From the biomechanical perspective, prolonged sitting may pose a high risk of lumbar disc degeneration, and therefore adjusting the posture properly in the early stage of sitting time may be useful to mitigate that. Additionally, upright sitting is a safer posture, while flexed sitting posture is more harmful.

Keywords: Lumbar intervertebral disc; Daily sitting postures; Finite element analysis; Poroelastic model

Biomechanical Response of Lumbar Intervertebral Disc in Daily Sitting Postures: A Poroelastic Finite Element Analysis

1. Introduction

Increasing sitting time is a global health problem, affecting people of all ages (Matusiak-Wieczorek et al. 2020), for which the World Health Organization has released relevant guidelines to highlight the importance of limiting sitting time to promote healthy sitting habits (Okely et al. 2021). It was reported that adults spent approximately half of the waking hours in sitting, equivalent to eight hours a day (Healy et al. 2011). Previous cross-sectional studies indicated that prolonged sitting in poor posture may increase the possibility of lumbar disc degeneration, which would further give rise to low back pain and deteriorate quality of life (Kanayama et al. 2009; Korshøj et al. 2018). However, the mechanistic link between sedentary behavior and disc degeneration is not fully clear, and more knowledge to understand the potential effect of different sedentary behaviors on the disc is necessary.

Intervertebral disc degeneration is a clinical degenerative disease closely related to mechanical loads (Adams and Roughley 2006). The disc sustains the compressive load for prolonged periods, exhibiting a creep behavior, where its compressive deformation often worsens (Adams et al. 1987; Adams et al. 1996). The increased deformation of the disc often causes higher stress, which may lead to mechanical damage accumulation and initiate the disc degeneration (Adams et al. 2000). Meanwhile, the disc gradually becomes less hydrated due to severe efflux of fluid (McMillan et al. 1996) and could have more significant elastic behavior than viscoelasticity. As a result, a declined energy dissipation capacity of the disc could lead to the increasing risk of disc failure (Jamison and Marcolongo 2014). Upright, flexed and extended sittings are three most common postures during daily life (Wong et al. 2019), and maintaining a sustained sitting posture over a prolonged period of time may put the disc under a physiologically-unfavorable mechanical environment, further increasing the likelihood of disc degeneration.

Finite element (FE) analysis is a cost-effective method to explore the etiology of intervertebral disc degeneration, which can provide mechanical interpretation to various loading scenarios (Hu et al. 2019). In contrast to the elastic FE models, the poroelastic FE models take into account the existence of deformable solid phase and, implicitly, the fluid in pore phase, thus allowing simulating the time-dependent behavior of the disc. Simon et al. (1985) were among the first to establish a poroelastic model to study creep response in a symmetrical spinal segment. Subsequently, poroelastic models were widely used to study the mechanical response of the disc under various loading conditions such as continuous load, vibration load, and shock load (Argoubi and Shirazi-Adl 1996; Cheung et al. 2003; Lee and Teo 2004; Schmidt et al. 2010; Qasim et al. 2012; Zanjani-Pour et al. 2016; Fan et al. 2018; Nikkhoo et al. 2018). Unfortunately, most studies simplified the loading conditions. Further exploration of disc response in daily postures was required. Zanjani-Pour et al. (2016) created a 2D lumbar spine poroelastic FE model and applied displacement boundary condition representing a specific sitting posture, but the authors indicated that employing a 2D model was likely to affect the accuracy of the predicted results. Additionally, our knowledge of the relationship between daily sitting postures and the disc degeneration is still poorly understood. Therefore, it is necessary to establish a 3D poroelastic model to investigate mechanical response of the lumbar disc under different sitting postures.

This study aims to establish and validate a 3D poroelastic lumbar FE model, where the time-dependent biomechanical response of the disc exposed to prolonged sitting and the effect of different sitting postures on the disc will be investigated.

2. Methods

2.1. The finite element model

The FE model was constructed based on CT images of a 25-year-old male volunteer in the supine posture without history of spinal diseases. The slice thickness of CT image was 0.625 mm, and the image resolution was 512×512. The cross-sectional area of our disc model was 1318 mm^2 within the range of previous measurement (Virk et al. 2021). The FE mesh was generated by Hypermesh 2020 (Altair, USA). The vertebral model consisted of cortical bone, cancellous bone, and bony posterior elements. A uniform thickness was assigned to the cortical bone. The structure of lumbar disc model was composed of cartilage endplates, nucleus pulposus, annulus fibrosus lamellae and inter-lamellar matrix (ILM). Annulus fibrosus lamellae were meshed by 22 concentric layers and the ILM was a cohesive structure located between adjacent annulus layers (Tavakoli and Costi 2018). The established FE model was shown in Figure 1.

2.2. Material properties

All structures were endowed with biphasic material properties except for the bony posterior elements. Linear elastic material was used to describe the solid phase material of cartilage endplates, cortical bone, cancellous bone, and bony posterior elements (Schmidt et al. 2006; Schmidt et al. 2010). The solid phase of the nucleus pulposus and ILM were assumed as hyper-elastic Neo-Hooke formulation (Mengoni et al. 2016; Fan et al. 2018). Annulus fibrosus lamellae represented as a fiber-reinforced composite with the Holzapfel-Gasser-Ogden material formulation (Holzapfel et al. 2005), which was defined by five parameters (C_{10}, D, k_1, k_2, *kappa*). For simplicity, the value of kappa was set to 0 for aligned fibers. Considering the variations of material properties, annulus fibrosus lamellae were divided into four major regions: anterior inner (AI), anterior outer (AO), posterior inner (PI), posterior outer (PO). There were two fiber families with $\pm 30°$ alternative orientation with respect to the horizontal plane, according to a previous study (Zhu et al. 2012).

$$U = C_{10}(\bar{I}_1 - 3) + \frac{1}{D}\left[\frac{(J^{el})^2 - 1}{2} - lnJ^{el}\right] + \frac{k_1}{2k_2}\sum_{\alpha=1}^{N}\left\{exp\left[k_2\bar{E}_\alpha{}^2\right] - 1\right\} \quad (1)$$

C_{10} affects the stiffness of the ground subatance. D affects the ground substance compression. k_1, k_2 determine the non-linear behavior of collagen fibers.

Fluid phase material properties were selected based on strain-dependent permeability formulation (Argoubi and Shirazi-Adl 1996).

$$k = k_0\left[\frac{e(1+e_0)}{e_0(1+e)}\right]^2 exp\left[M\left(\frac{1+e}{1+e_0} - 1\right)\right] \quad (2)$$

The permeability k varies with voids ratio e. Different structures have specific initial voids ratio e_0 and initial permeability k_0. M is an experimental matching factor.

$$e = \frac{\Phi_f}{1-\Phi_f} \quad (3)$$

Φ_f is the porosity of the tissue, which is dependent on the tissue deformation.

$$\Phi_f = 1 - J^{-1}(1 - \Phi_{f0}) \quad (4)$$

Where J is the ratio of the medium volume in the current configuration to its volume in the reference configuration.

Seven major ligaments existing in the lumbar spine were represented by connector elements. The tensile-only behavior of the ligaments was described by non-linear curves (Zhu et al. 2012). The viscoelastic properties of ligaments were neglected in this study, which only played a role in the early stage of loading and had little effect on the long-term predicted mechanical response (Lee and Teo 2004). The initial gap of the facet articular cartilage layer was 0.5 mm. The same exponential contact algorithm as Schmidt et al. (2010) was used to simulate mechanical role of articular cartilage. The vertebral body and lumbar disc were connected by "tie" interaction property, which made the degrees of freedom on the corresponding nodes equal. The material properties of the different structures were summarized in Table 1.

2.3. Validation

To verify the accuracy of the established FE model, different validation tests were performed.

1) FE model generated in this study was imposed with combined loading modes consisting of 7.5 Nm flexion, extension, lateral bending, and axial rotation respectively under a 500 N compressive load. For range of motion (RoM), simulation results obtained in the current study were compared with the experimental results reported by Heuer et al. (2007).

2) To validate time-dependent behavior of the disc, an axial load of 1000 N was applied to the model for 8 hours. Temporal variations of the disc height loss were compared with in vitro experimental results (Adams et al. 1987; Adams et al. 1996).

3) The model was subjected to compressive loads of 100 N, 500 N and 1000 N simulating equivalent compressive loads on supine, standing and moderate activity, respectively (Rohlmann et al. 2009; Schmidt et al. 2010; Fan et al. 2015). The predicted intradiscal pressure was compared with available values in vivo and vitro experiments (Adams et al. 1996; Wilke et al. 1999).

2.4. Boundary and loading conditions

All degrees of freedom on the inferior surface of L5 were constricted. To simulate the osmotic behavior of the disc, a constant 0.25 MPa boundary pore pressure was imposed on all external surfaces on the spine (Schmidt et al. 2010). In this study, the loading conditions were defined as four different cases: 1) a constant compressive load of 500 N simulating standing (Rohlmann et al. 2009), 2) a higher compressive load of 700 N representing upright sitting (Nachemson 1966), 3) a compressive load of 900 N with 2° flexion was taken as a flexed sitting posture (Nachemson 1966; Claus et al. 2016), 4) a compressive load of 900 N with 2° extension was characterized as an extended sitting posture (Bae and Mun 2010; Claus et al. 2016). Four loading conditions represented different daily postures lasting 8 hours. The compressive load was applied using the follower load technique. The path of the follower load was along spinal curvature, remaining the loading direction continuously perpendicular to the disc plane, which could minimize the intervertebral angle (Shirazi-Adl and Parnianpour 2000; Rohlmann et al. 2009). The rotation angle was applied to a reference point coupling to the superior surface of L4. All the above simulations were analyzed using FE software ABAQUS 6.14 (Dassault Systèmes, Vélizy-Villacoublay, France).

3. Results

3.1. Validation results

As for RoM, the predicted values were 7.0°, 3.4°, 4.1°, and 2.0°, respectively, as shown in Figure 2a. The values were all within the range of those measured for lumbar segment specimens and showed a good agreement with in vitro experimental results (Heuer et al. 2007).

In Adams's experiments, the measurements indicated the disc height loss of 1.2 ± 0.3 mm after 2–3 h and 1.53 ± 0.34 mm after 6 h (Adams et al. 1987; Adams et al. 1996). Under the consistent loading conditions, the predicted the loss of disc height was 1.41 mm after 2 h and 1.65 mm after 6 h in current FE model (Figure 2b).

Intradiscal pressure served as an important indicator for evaluating biomechanical properties of the disc. The simulation results showed that intradiscal pressure respectively averaged at 0.10 MPa, 0.50 MPa and 0.95 MPa in supine, standing and moderate activity (Figure 2c), which kept a great consistency with in vivo and in vitro measurement results (Adams et al. 1996; Wilke et al. 1999). Results showed that the predicted intradiscal pressure and the applied loads exhibited an approximate positive linear regression relationship. All validations above illustrated the accuracy of the established FE model, and it could be applied to the following daily postures loading simulations.

3.2. Daily postures analysis

To investigate time-dependent response of the disc in different daily postures, the temporal variations of disc height loss, fluid loss in the nucleus pulposus, intradiscal pressure and von-Mises stress in ILM were analyzed in this study.

The disc axial deformation under the various loading conditions is shown in Figure 3a. The disc height loss was represented by the axial displacement at the center point of the upper endplate. And the loss of disc height in flexed and extended sitting was due to the contribution of both compressive load and rotation. The decreased height of the disc increased with time gradually. The original height of the intervertebral disc was 10.17 mm. After 8 hours, the disc height reduced by 10.5%, 13.6%, 16.3%, and 13.6% in the four daily postures, respectively. Also, it illustrated the decreasing trend of the disc height change rate and a greater rate appeared in the early stage of the loading. The height loss in flexed sitting was significantly higher than those generated by other daily postures.

The fluid loss in the nucleus pulposus increased with time and differed from loading cases (Figure 3b). This parameter was expressed as a percentage of the total initial fluid content. At the end of the loading, the nucleus lost 6.2% in standing, 10.2% in upright sitting, 13.6% in flexed sitting and 10.8% in extended sitting of water content, respectively. The fluid loss in the flexed sitting posture maintained at a relatively high level during the entire loading process. And it could be seen that more fluid loss occurred in the first few hours.

The change of intradiscal pressure for all cases were shown in Figure 3c. Intradiscal pressure was presented by the average pore pressure in the nucleus pulposus. Under different loading cases, the maximum intradiscal pressure was found in standing (0.50 MPa), upright sitting (0.68 MPa), flexed sitting (0.87 MPa) and extended sitting (0.77 MPa) at the initial loading stage. Gradually, the predicted values dissipated noticeably with time. The minimum values were predicted 0.35 MPa in standing, 0.46 MPa in upright sitting, 0.59 MPa in flexed sitting and 0.46 MPa in extended sitting after 8 hours loading.

The von-Mises stress in the ILM increased with time slightly in all simulations (Figure 3d). This predicted value was calculated by dividing the sum of von-Mises stress by the total number of elements in the ILM. Also, it showed that the stress changes were mainly affected by the different loading conditions.

3.3. Comparison of four daily postures

To compare the effect of four different daily postures on the intervertebral disc, the von-Mises stress distributions of ILM were predicted and relative values of relevant biomechanical parameters were calculated.

After 8 hours of different daily postures, the detailed von-Mises stress distributions of ILM were displayed in Figure 4. The stress concentration occurred in the posterior region while standing, upright sitting and extended sitting. In the flexed sitting posture, the stress concentration was located close to the anterior region. The maximum von-Mises stress in the four postures of standing, upright sitting, flexed sitting, and extended sitting was 0.28 MPa, 0.42 MPa, 0.51 MPa and 0.65 MPa, respectively.

At the end of the loading, the relative values of biomechanical parameters with respect to the predicted values during standing were summarized (Figure 5). It was apparent that the predicted values in standing were lower than sitting. Among all predicted mechanical results, the maximum values completely presented in the flexed sitting. The loss of disc height up to 156% of the reference value was found in the flexed sitting. The fluid loss, 219% of the reference value, was found in the flexed sitting and the values of 163% and 174% were separately observed in the upright sitting and extended sitting. In the study of intradiscal pressure, the relative values calculated in the three sitting postures were 131%, 168%, and 132%, respectively. For each loading conditions, the average von-Mises stress increased in the following order: standing, upright sitting, extended sitting and flexed sitting. The relative value of average von-Mises stress was 149% in the flexed sitting, significantly greater than that of the standing posture.

4. Discussion

It is important to understand the role of sedentary behavior on the spine, as long-term loading may affect the spinal structures and initiate degeneration of the disc. In FE studies, there is lack of quantitative data on the time-dependent response of the disc under sitting loads simulating an upright sitting posture, a flexed or extended sitting posture.

A 3D poroelastic finite element model of a lumbar motion segment was developed and validated first. This study then discussed the influence of different sitting postures and its duration on the mechanical response of the disc. It was found that the incidence of disc degeneration at L4/L5 spinal segment was relatively high, and sedentary behavior was also related to the pathological symptoms of disc at this segment (Kanayama et al. 2009). Therefore, the FE model of L4/L5 spinal segment was established in this study. The incorporation of permeability material properties is the primary advantage of this model, which could help better understand how mechanical response of the disc changes over time. And such time-dependent response can be explained, at least in part, by the motion of fluid content in the disc when loaded. The developed FE model has been examined for its validity against axial displacement, intradiscal pressure and RoM obtained in the experiments. Regarding the loading conditions, 500 N compressive load represented the standing condition as a control (Rohlmann et al. 2009). Upright sitting increased loads by nearly 40% loads in comparison with standing (Nachemson 1966). According to multiple studies, flexed sitting posture would exert 900 N force on the lumbar spine and there existed little difference in the compressive load under flexed or extended sitting (Nachemson 1966; Bae and Mun 2010). The selected ± 2° angle represented the daily change in sitting postures, and this value came from the measurement of the lumbar spine angle (Claus et al. 2016). Sagittal spine motion was dominant in sitting postures, while the mechanical effect of other plane motions such as lateral bending and axial rotation was weak, so we focused on its sagittal effect (Berry et al. 2019). Meanwhile, the simulation time of 8 hours was in line with the living habits of modern people.

The disc lost 12.3% of its height under 700 N for four hours. This value was relatively consistent with the cumulative height loss of 13.5% under the same loading amplitude and time (Adams and Hutton 1983). As indicated by the slope of the curve, the predicted height loss was rapid in initial few hours but much slower by the end of the loading (Figure 3a). Previous studies proved that due to the poroelastic nature of the disc, the creep compression deformation was related to the fluid loss of the disc (Adams and Hutton 1983). So, we assumed that the predicted varying rate could be explained by the variation of water content in the intervertebral disc (Figure 3b). To some extent, under the sustained compressive load, the intervertebral disc experienced a large amount of fluid loss, especially from the highly hydrated nucleus pulposus. Consequently, the dehydrated disc would exhibit less time-dependent behavior, more elastic mechanical properties, and gradually became stiffer.

Our model predicted 6.5% fluid loss in the nucleus under 700 N creep loading after four hours. This value approximately agreed with prediction of 5% fluid loss measured by Adams and Hutton (1983). Some studies showed that proper fluid exchange was conducive to the metabolic activity throughout the entire disc (McMillan et al. 1996; Cheung et al. 2003). Meanwhile, the water content in the disc was also responsible to creep response, and shock absorption function. Jamison and Marcolongo (2014) demonstrated a large amount of fluid loss was accompanied by higher instability and energy dissipation, thereby increasing the risk of intervertebral disc failure. Our simulation results showed that the predicted fluid loss increased with loading time. Therefore, from the biomechanical perspective, it implied that the sitting time might was related to the risk of intervertebral disc degeneration and long sitting time increased the risk of disc degeneration. Moreover, more significant fluid loss occurred in the first few hours. This meant that proper posture adjustments were desired in the early stages of sitting, which could avoid the continuous fluid loss of the disc due to the fixed posture.

Intradiscal pressure during daily postures has been measured in a few previous studies. Our predicted intradiscal pressure in upright, flexed and extended sitting postures was consistent with the values reported by Sato et al. (1999). The water in the nucleus pulposus played an important role in sharing the external load, which was expressed by the magnitude of intradiscal pressure. As a result, the gradually decreasing intradiscal pressure was accompanied with a simultaneous increasing fluid loss in the nucleus pulposus. This indicated the load-bearing effect of the nucleus pulposus was weakened and the more loads would be transferred to adjacent structures. The current finding was consistent with the result of published studies that, over time, the annulus fibrosus would be subjected to a greater compressive load than the nucleus, and annulus was a common site of compressive failure under sedentary posture (Argoubi and Shirazi-Adl 1996). In other words, prolonged sitting would weaken the carrying capacity of the nucleus pulposus, change the distribution of mechanical loads on the disc, and could cause degeneration in the intervertebral disc.

ILM was previously reported to have an important role in providing annulus fibrosus lamellae connectivity (Tavakoli and Costi 2018; Tavakoli et al. 2018). High stress in the ILM contributed to the delamination of the annulus fibrosus, providing a potential mechanism for the protrusion of nucleus (Gregory et al. 2014). The von-Mises stress distribution in the ILM (Figure 4) showed that the stress mainly concentrated in the posterior of the disc, while standing, upright sitting and extended sitting. Such analysis indicated that the posterior ILM experienced more force than other regions and there was a greater risk of delamination failure at the posterior annulus, in good agreement with a previous study (Qasim et al. 2012). Additionally, our findings also supported the clinical observation that the herniated disc mainly appeared in the posterior region of the disc.

The simulation results revealed that the response of the lumbar mechanical parameters in four daily postures were drastically different, as shown in Figure 5. The predicted values in sitting postures were significantly greater than those in standing posture, which confirmed the general perception of orthopedists and physiotherapists (Lord et al. 1997). Since the annulus fibers were tensioned by intradiscal pressure, it was generally believed that higher intradiscal pressure was associated with a higher risk of annulus rupture and disc degeneration (Chu et al. 2018). Thus, it could be concluded that sitting for a long time was more harmful to the disc than standing. This finding supported the follow-up study that showed a stronger correlation between low back pain and sedentary work (Lunde et al. 2017). Wilke et al. (1999) reported that standing and sitting had similar effect on intradiscal pressure, which was inconsistent with the results of this study and weakened the reliability. This may need further large scale in vivo measurements for discussion. Moreover, the results showed that although the same compressive load was applied in the flexed and extended sitting postures, the relative values of the flexed sitting posture was much greater. It could be assumed that the angle of flexion exerted additional loads to the disc. This might be the reason for larger deformation, higher stress, and more fluid loss were observed in the flexed sitting posture. The same phenomenon was reported by Adams and Hutton (1983) that the disc expelled more fluid and intradiscal pressure was greater when the motion segment was flexed. Thus, it’s indicated that flexed sitting posture was much more harmful than the other two sitting postures, and prolonged flexed sitting should be especially avoided in our daily life. Interestingly, similar biomechanical parameters were obtained in the upright and extended sitting postures. However, the maximum von-Mises stress in the extended sitting posture was 0.65 MPa in the posterior region of ILM, while the value in upright sitting was 0.42 MPa, as illustrated in Figure 4. This could be due to the fact that the extended sitting posture led to more load in the posterior region of the ILM, which posed a greater risk of annulus damage. Therefore, upright sitting posture appeared to have the least adverse effect on the disc and could be considered a relatively safe daily sitting posture.

There were some simplifications in the current study. Firstly, no experimental data of the permeability parameters of ILM has been reported. Therefore, their material parameters were assumed to be the same as those of fibrous lamellae. Secondly, the muscle was not modelled in the established FE model. The spinal ligaments pretension was neglected, but the previous research showed that this simplification had little effect on predicted disc stress (Hortin and Bowden 2016). In studies where ligament stress is the primary output, the role of ligament pretension must be considered. Using CT taken at supine posture will affect the curvature of the model and the load in standing and upright sitting to some degree. However, the establishment of a single-segment model and the application of follower load could alleviate the influence. Applying simplified loads to define sitting postures may not be realistic enough, but the combination of follower load and rotation could achieve a certain degree of mechanical effect. Fixed pore pressure to simulate osmotic pressure was another limitation. Although this approach has been successfully adopted in previous studies (Schmidt et al. 2010; Galbusera et al. 2011; Fan et al. 2018), a more realistic description of osmotic pressure is still necessary. A model describing the osmotic potential with a three-phase fully coupled approach is needed in further study. Above simplifications were involved, but to a certain extent, the validation tests illustrated the accuracy of established FE model.

5. Conclusions

From the biomechanical perspective, prolonged sitting may pose a high risk of lumbar disc degeneration, and therefore adjusting the posture properly in the early stage of sitting time may be useful to mitigate that. Additionally, upright sitting is a safer posture, while flexed sitting posture is more harmful.

Declaration of Competing Interest

None of the authors have any conflict of interest.

Acknowledgements

This work was supported by National Key R&D Program of China (No. 2020YFC2008703), Shanghai Clinical Research Center for Aging and Medicine (19MC1910500) and Newton Fund (UK-China Joint Research and Innovation Partnership Fund - 440004097). Liang-dong Zheng, Yu-ting Cao and Yi-ting Yang contribute equally to this paper.

References

Adams MA, Dolan P, Hutton WC. 1987. Diurnal variations in the stresses on the lumbar spine. Spine. 12(2):130–137.

Adams MA, Freeman B, Morrison HP, Nelson IW, Dolan P. 2000. Mechanical initiation of intervertebral disc degeneration. Spine. 25(13):1625–1636.

Adams MA, Hutton WC. 1983. The Effect of Posture on the Fluid Content of Lumbar Intervertebral Discs. Spine. 8(6):665–671.

Adams MA, McMillan DW, Green TP, Dolan P. 1996. Sustained loading generates stress concentrations in lumbar intervertebral discs. Spine. 21(4):434–438.

Adams MA, Roughley PJ. 2006. What is Intervertebral Disc Degeneration, and What Causes It. Spine. 31(18):2151–2161.

Argoubi M, Shirazi-Adl A. 1996. Poroelastic creep response analysis of a lumbar motion segment in compression. Journal of Biomechanics. 29(10):1331–1339.

Bae TS, Mun M. 2010. Effect of lumbar lordotic angle on lumbosacral joint during isokinetic exercise: a simulation study. Clinical Biomechanics. 25(7):628–635.

Berry DB, Hernandez A, Onodera K, Ingram N, Ward SR, Gombatto SP. 2019. Lumbar spine angles and intervertebral disc characteristics with end-range positions in three planes of motion in healthy people using upright MRI. Journal of Biomechanics. 89:95–104.

Cheung JTM, Zhang M, Chow DHK. 2003. Biomechanical responses of the intervertebral joints to static and vibrational loading: a finite element study. Clinical Biomechanics. 18(9):790–799.

Chu G, Shi C, Lin J, Wang S, Wang H, Liu T, Yang H, Li B. 2018. Biomechanics in Annulus Fibrosus Degeneration and Regeneration. In: Chun HJ, Park CH, Kwon IK, Khang G, editors. Cutting-Edge Enabling Technologies for Regenerative Medicine

[Internet]. Vol. 1078. Singapore: Springer Singapore; [accessed 2022 Nov 24]; p. 409–420.

Claus AP, Hides JA, Moseley GL, Hodges PW. 2016. Thoracic and lumbar posture behaviour in sitting tasks and standing: Progressing the biomechanics from observations to measurements. Appl Ergon. 53 Pt A:161–168.

Fan R, Gong H, Qiu S, Zhang X, Fang J, Zhu D. 2015. Effects of resting modes on human lumbar spines with different levels of degenerated intervertebral discs: a finite element investigation. BMC Musculoskelet Disord. 16:221.

Fan RX, Liu J, Li YL, Liu J, Gao JZ. 2018. Finite Element Investigation of the Effects of the Low-Frequency Vibration Generated by Vehicle Driving on the Human Lumbar Mechanical Properties. Biomed Res Int. 2018:7962414.

Galbusera F, Schmidt H, Noailly J, Malandrino A, Lacroix D, Wilke HJ, Shirazi-Adl A. 2011. Comparison of four methods to simulate swelling in poroelastic finite element models of intervertebral discs. J Mech Behav Biomed Mater. 4(7):1234–1241.

Gregory D, Bae WC, Sah RL, Masuda K. 2014. Disc degeneration reduces the delamination strength of the annulus fibrosus in the rabbit annular disc puncture model. Spine Journal. 14(7):1265–1271.

Healy GN, Matthews CE, Dunstan DW, Winkler E. 2011. Sedentary time and cardio-metabolic biomarkers in US adults: NHANES 2003–06. European Heart Journal. 32(5):590–597.

Heuer F, Schmidt H, Klezl Z, Claes L, Wilke H-J. 2007. Stepwise reduction of functional spinal structures increase range of motion and change lordosis angle. Journal of Biomechanics. 40(2):271–280.

Holzapfel GA, Schulze-Bauer C, Feigl G, Regitnig P. 2005. Single lamellar mechanics of the human lumbar anulus fibrosus. Biomechanics & Modeling in Mechanobiology. 3(3):125–140.

Hortin MS, Bowden AE. 2016. Quantitative comparison of ligament formulation and pre-strain in finite element analysis of the human lumbar spine. Comput Methods Biomech Biomed Engin. 19(14):1505–1518.

Hu B-W, Lv X, Chen S-F, Shao Z-W. 2019. Application of Finite Element Analysis for Investigation of Intervertebral Disc Degeneration: from Laboratory to Clinic. Curr Med Sci. 39(1):7–15.

Jamison D, Marcolongo MS. 2014. The effect of creep on human lumbar intervertebral disk impact mechanics. Journal of Biomechanical Engineering. 136(3):031006.

Kanayama M, Togawa D, Takahashi C, Terai T, Hashimoto T. 2009. Cross-sectional magnetic resonance imaging study of lumbar disc degeneration in 200 healthy individuals. J Neurosurg Spine. 11(4):501–507.

Korshøj M, Hallman DM, Mathiassen SE, Aadahl M, Holtermann A, Jørgensen MB. 2018. Is objectively measured sitting at work associated with low-back pain? A cross sectional study in the DPhacto cohort. Scandinavian Journal of Work, Environment & Health. 44(1):96–105.

Lee KK, Teo EC. 2004. Poroelastic analysis of lumbar spinal stability in combined compression and anterior shear. Journal of Spinal Disorders & Techniques. 17(5):429–438.

Lord MJ, Small JM, Dinsay JM, Watkins RG. 1997. Lumbar lordosis. Effects of sitting and standing. Spine (Phila Pa 1976). 22(21):2571–2574.

Lunde LK, Koch M, Knardahl S, Bo V. 2017. Associations of objectively measured sitting and standing with low-back pain intensity: a 6-month follow-up of construction and healthcare workers. Scandinavian Journal of Work Environment & Health. 43(3):269–278.

Matusiak-Wieczorek E, Lipert A, Kochan E, Jegier A. 2020. The time spent sitting does not always mean a low level of physical activity. BMC Public Health. 20(1):317.

McMillan DW, Garbutt G, Adams MA. 1996. Effect of sustained loading on the water content of intervertebral discs: Implications for disc metabolism. Annals of the Rheumatic Diseases. 55(12):880–887.

Mengoni M, Jones AC, Wilcox RK. 2016. Modelling the failure precursor mechanism of lamellar fibrous tissues, example of the annulus fibrosus. Journal of the Mechanical Behavior of Biomedical Materials. 63:265–272.

Nachemson A. 1966. The Load on Lumbar Disks in Different Positions of the Body: Clinical Orthopaedics and Related Research. 45(1):107–122.

Nikkhoo M, Wang JL, Parnianpour M, El-Rich M, Khalaf K. 2018. Biomechanical response of intact, degenerated and repaired intervertebral discs under impact loading - Ex-vivo and In-Silico investigation. J Biomech. 70:26–32.

Okely AD, Kontsevaya A, Ng J, Abdeta C. 2021. 2020 WHO guidelines on physical activity and sedentary behavior. Sports Medicine and Health Science. 3(2):115–118.

Qasim M, Natarajan RN, An HS, Andersson GB. 2012. Initiation and progression of mechanical damage in the intervertebral disc under cyclic loading using continuum damage mechanics methodology: A finite element study. J Biomech. 45(11):1934–1940.

Rohlmann A, Zander T, Rao M, Bergmann G. 2009. Applying a follower load delivers realistic results for simulating standing. J Biomech. 42(10):1520–1526.

Sato K, Kikuchi S, Yonezawa T. 1999. In vivo intradiscal pressure measurement in healthy individuals and in patients with ongoing back problems. Spine (Phila Pa 1976). 24(23):2468–2474.

Schmidt H, Heuer F, Simon U, Kettler A, Rohlmann A, Claes L, Wilke HJ. 2006. Application of a new calibration method for a three-dimensional finite element model of a human lumbar annulus fibrosus. Clinical Biomechanics. 21(4):337–344.

Schmidt H, Shirazi-Adl A, Galbusera F, Wilke HJ. 2010. Response analysis of the lumbar spine during regular daily activities--a finite element analysis. J Biomech. 43(10):1849–1856.

Shirazi-Adl A, Parnianpour M. 2000. Load-bearing and stress analysis of the human spine under a novel wrapping compression loading. Clin Biomech (Bristol, Avon). 15(10):718–725.

Simon BR, Wu JSS, Carlton MW, Evans JH, Kazarian LE. 1985. Structural models for human spinal motion segments based on a poroelastic view of the intervertebral disk. Journal of Biomechanical Engineering-Transactions of the Asme. 107(4):327–335.

Tavakoli J, Amin DB, Freeman BJC, Costi JJ. 2018. The Biomechanics of the Inter-Lamellar Matrix and the Lamellae During Progression to Lumbar Disc Herniation: Which is the Weakest Structure? Ann Biomed Eng. 46(9):1280–1291.

Tavakoli J, Costi JJ. 2018. New findings confirm the viscoelastic behaviour of the inter-lamellar matrix of the disc annulus fibrosus in radial and circumferential directions of loading. Acta Biomater. 71:411–419.

Virk S, Meyers KN, Lafage V, Maher SA, Chen T. 2021. Analysis of the influence of species, intervertebral disc height and Pfirrmann classification on failure load of an injured disc using a novel disc herniation model. Spine J. 21(4):698–707.

Wilke HJ, Neef P, Caimi M, Hoogland T, Claes LE. 1999. New in vivo measurements of pressures in the intervertebral disc in daily life. Spine (Phila Pa 1976). 24(8):755–762.

Wong AYL, Chan TPM, Chau AWM, Tung Cheung H, Kwan KCK, Lam AKH, Wong PYC, De Carvalho D. 2019. Do different sitting postures affect spinal biomechanics of asymptomatic individuals? Gait Posture. 67:230–235.

Zanjani-Pour S, Winlove CP, Smith CW, Meakin JR. 2016. Image driven subject-specific finite element models of spinal biomechanics. Journal of Biomechanics. 49(6):919–925.

Zhu R, Cheng LM, Yu Y, Zander T, Chen B, Rohlmann A. 2012. Comparison of four reconstruction methods after total sacrectomy: A finite element study. Clinical Biomechanics. 27(8):771–776.

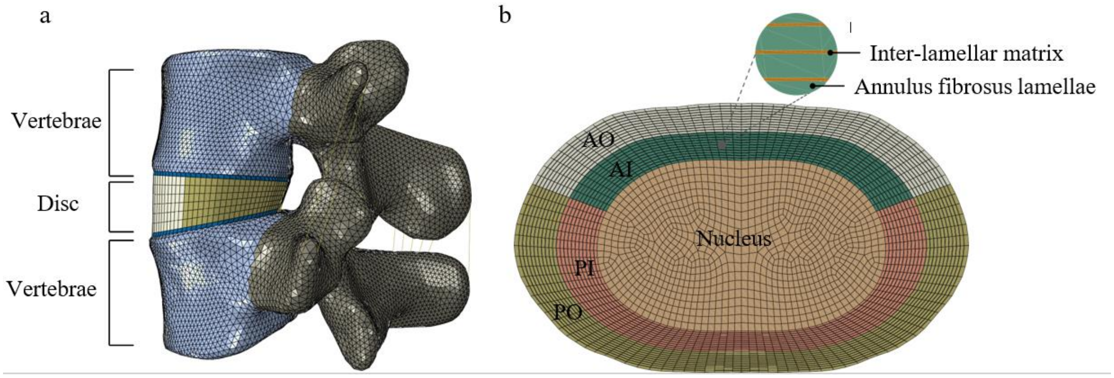

Figure 1. (a) Established finite element L4-L5 model. (b) Detailed view of the intervertebral disc including nucleus, inter-lamellar matrix, and divisions of the annulus fibrosus lamellae.

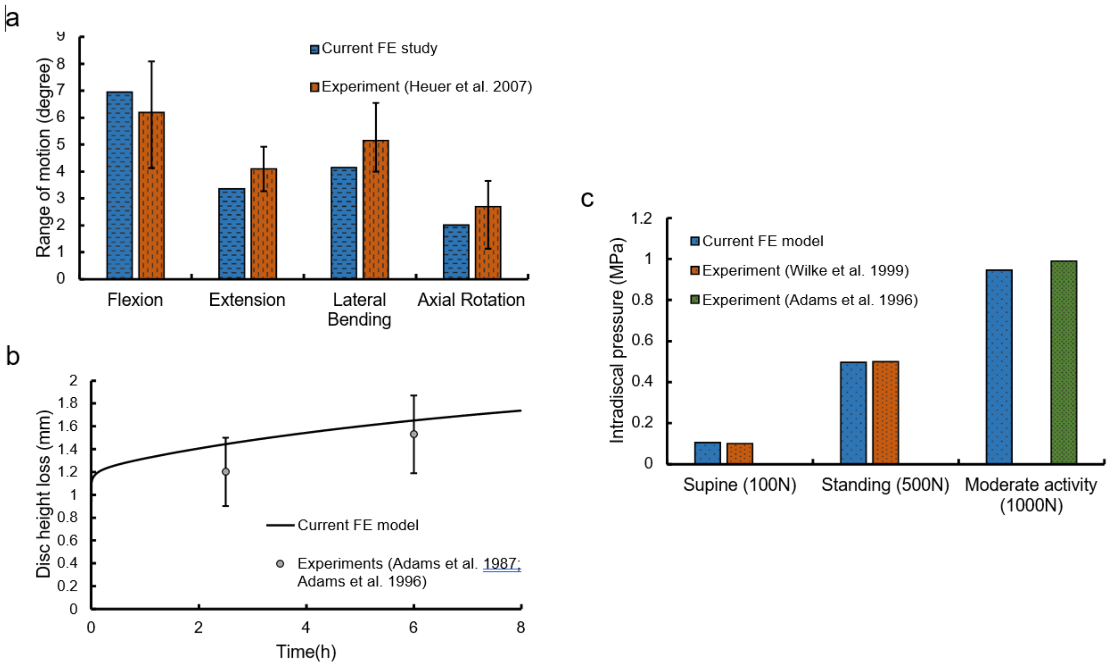

Figure 2. (a) Comparison of range of motion with current FE model and experimental results from Heuer et al. (2007). (b) The predicted disc height loss in comparison to the experimental measurements in the literatures (Adams et al. 1987; Adams et al. 1996). (c) Comparison of intradiscal pressure in current FE model with and experimental results from Adams et al. (1996) as well as Wilke et al. (1999).

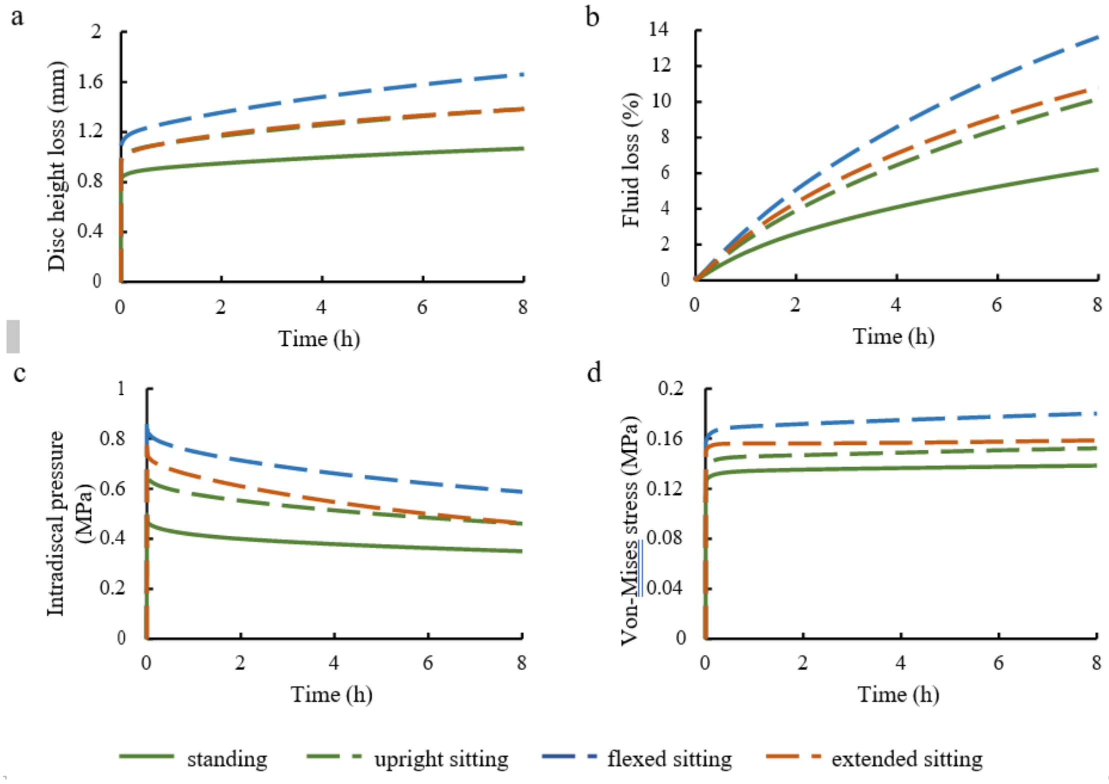

Figure 3. Temporal variations of (a) disc height loss, (b) fluid loss, (c) intradiscal pressure, (d) von-Mises stress.

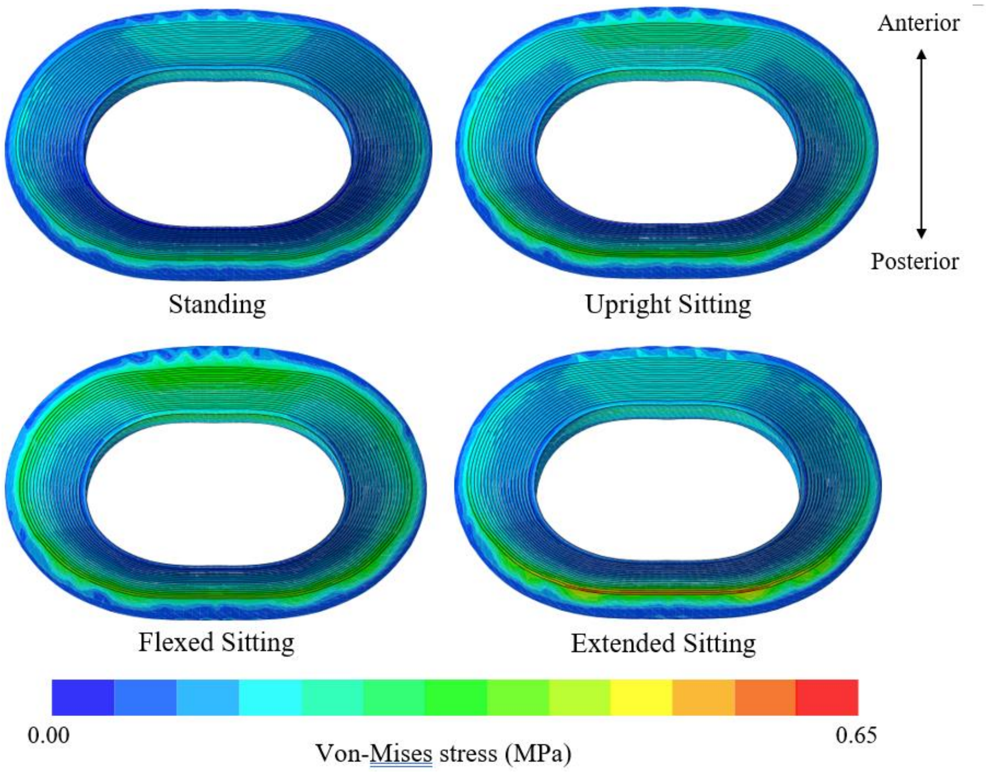

Figure 4. Von-Mises stress distributions of ILM at the time of 8 h during different daily postures.

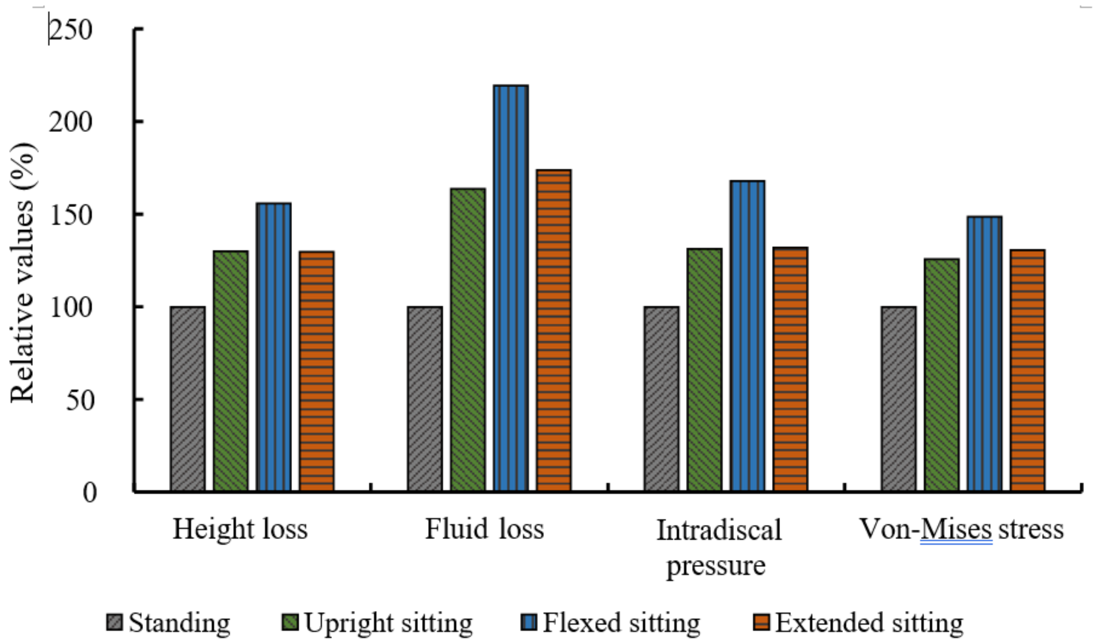

Figure 5. Relative values of predicted parameters for the four daily postures

Table 1 Biphasic Material properties employed in the FE model.

<table>
<tr><th rowspan="2">Structure</th><th rowspan="2">Element type</th><th rowspan="2" colspan="5">Solid phase material</th><th colspan="3">Fluid phase material</th><th rowspan="2">References</th></tr>
<tr><th>Initial permeability
k_0 ($m^4N^{-1}s^{-1}$)</th><th>Initial voids ratio
e_0</th><th>M</th></tr>
<tr><td>Nucleus pulposus</td><td>C3D8P</td><td colspan="5">Neo-Hookean
$C_{10} = 0.125$ MPa, $D = 2.475$ MPa^{-1}</td><td>3.0×10^{-16}</td><td>4.00</td><td>10.0</td><td>(Argoubi and Shirazi-Adl 1996; Fan et al. 2018)</td></tr>
<tr><td>Inter-lamellar matrix</td><td>C3D8P</td><td colspan="5">Neo-Hookean
$C_{10} = 0.0671$ MPa, $D = 0.2998$ MPa^{-1}</td><td>3.0×10^{-16}</td><td>2.33</td><td>12.0</td><td>(Argoubi and Shirazi-Adl 1996; Mengoni et al. 2016)</td></tr>
<tr><td rowspan="6">Annulus fibrosus lamellae</td><td rowspan="6">C3D8P</td><td colspan="5">Holzapfel-Gasser-Ogden</td><td rowspan="6">3.0×10^{-16}</td><td rowspan="6">2.33</td><td rowspan="6">12.0</td><td rowspan="6">(Argoubi and Shirazi-Adl 1996; Holzapfel et al. 2005)</td></tr>
<tr><td></td><td>C_{10} (MPa)</td><td>D (MPa^{-1})</td><td>k_1</td><td>k_2</td></tr>
<tr><td>AO</td><td rowspan="4">0.11</td><td rowspan="4">0.545</td><td>6.1462</td><td>368.1053</td></tr>
<tr><td>AI</td><td>0.8144</td><td>40.6295</td></tr>
<tr><td>PO</td><td>1.4898</td><td>67.5292</td></tr>
<tr><td>PI</td><td>0.0725</td><td>14.5348</td></tr>
<tr><td>Cartilaginous endplate</td><td>C3D8P</td><td colspan="5">Linear
$E = 23.8$ MPa, $v = 0.4$</td><td>7.0×10^{-15}</td><td>4.00</td><td>10.0</td><td>(Argoubi and Shirazi-Adl 1996; Schmidt et al. 2006)</td></tr>
<tr><td>Cancellous bone</td><td>C3D4P</td><td colspan="5">Linear
$E = 100$ MPa, $v = 0.2$</td><td>1.0×10^{-13}</td><td>0.40</td><td>18.0</td><td>(Argoubi and Shirazi-Adl 1996; Schmidt et al. 2010)</td></tr>
<tr><td>Cortical bone</td><td>C3D6P</td><td colspan="5">Linear
$E = 10000$ MPa, $v = 0.3$</td><td>1.0×10^{-20}</td><td>0.02</td><td>22.0</td><td>(Argoubi and Shirazi-Adl 1996; Schmidt et al. 2010)</td></tr>
<tr><td>Bony posterior elements</td><td>C3D4</td><td colspan="5">Linear
$E = 3500$ MPa, $v = 0.25$</td><td>–</td><td>–</td><td>–</td><td>(Schmidt et al. 2006)</td></tr>
<tr><td>Ligaments</td><td>Connector</td><td colspan="5">Non-linear no compression</td><td>–</td><td>–</td><td>–</td><td>(Zhu et al. 2012)</td></tr>
</table>